

Nuclear Physics with Electroweak Probes

Carlotta Giusti

*Dipartimento di Fisica Nucleare e Teorica, Università degli Studi,
and INFN, Sezione di Pavia, via Bassi 6 I-27100 Pavia, Italy*

The research activities carried out in Italy during the last two years in the field of theoretical nuclear physics with electroweak probes are reviewed. Different models for electron-nucleus and neutrino-nucleus scattering are compared. The results obtained for electromagnetic reactions on few-nucleon systems and on complex nuclei are discussed. The recent developments in the study of electron- and photon-induced reactions with one and two-nucleon emission are presented.

I. INTRODUCTION

Several decades of theoretical and experimental investigation in the field of nuclear physics with electromagnetic probes have yielded a wealth of information on nuclear structure and interaction mechanisms [1]. An important contribution has been given by the Italian theory groups that since many years have been working in the field, within many international collaborations and in close connection with the experimental activities.

In spite of so many years of investigation and of the great progress achieved, some interesting aspects are still unclear and there is yet much to be learned. In the last few years theories have improved remarkably but some data are old, incomplete or not accurate enough to disentangle interesting effects. The need of a more complete experimental program to investigate nuclei with electromagnetic probes was already pointed out by G. Co' in the previous report two years ago [2].

In recent years almost all the Italian groups working in electron scattering have applied their models to ν -nucleus scattering. Although the two situations are different, the extension to neutrino scattering of the electron scattering formalism is straightforward. Moreover, electron scattering is the best available guide to determine the prediction power of a nuclear model.

The observation of neutrino oscillations and the proposal and realization of new experiments, aimed at determining neutrino properties with high accuracy, renewed interest in neutrino scattering on complex nuclei. In fact, neutrinos are elusive particles. They are chargeless, almost massless, and only weakly interacting. Their presence can only be inferred detecting the particles they create when colliding or interacting with matter. Nuclei are often used as neutrino detectors providing relatively large cross sections. The interest in ν -nucleus scattering extends to different fields, such as astrophysics, cosmology, particle and nuclear physics. In hadronic and nuclear physics neutrinos can excite nuclear modes inaccessible in electron scattering, can give information on the hadronic weak current and on the strange nucleon form factors [3]. Thus, neutrino physics is of great interest and involves many different phenomena. The interpretation of data, however, requires a detailed knowledge of the ν -nucleus interaction as well as reliable cross section calculations where nuclear effects are properly taken into account.

The different models used to treat electron- and ν -nucleus scattering are discussed in Sec. 2. The treatment of the two-body weak axial current is presented in Sec. 3. Scaling and superscaling in lepton-nucleus scattering are considered in Sec. 4. Electromagnetic reactions in few-body and complex nuclei are reviewed in Sects. 5 and 6, respectively.

II. ELECTRON-NUCLEUS AND NEUTRINO-NUCLEUS SCATTERING

Lepton-nucleus scattering is usually described in the one-boson exchange approximation. The exchanged boson is the photon in the case of the electromagnetic interaction and the Z^0 or W^\pm in the case of the weak interaction. In electron scattering the invariant amplitude is given by the sum of the one-photon and the one- Z^0 boson exchange term. The first term is parity conserving and the second one is Parity Violating (PV). PV Electron Scattering (PVES) requires a polarized incident electron and is interesting to study the strange nucleon form factors [3]. In ν ($\bar{\nu}$)-nucleus scattering the boson exchanged is the Z^0 for neutral-current (NC) scattering, i.e., (ν, ν') [$(\bar{\nu}, \bar{\nu}')$], and the W^+ (W^-) for charged-current (CC) scattering, where a charged lepton is obtained in the final state, i.e., (ν, l^-) [$(\bar{\nu}, l^+)$].

Different processes can thus be considered. In any case, in the one-boson exchange approximation, the cross section is given in the form

$$d\sigma = K L^{\mu\nu} W_{\mu\nu}, \quad (1)$$

where K is a kinematical factor, the lepton tensor $L^{\mu\nu}$ depends only on the lepton kinematics, and the nuclear response is contained in the hadron tensor $W^{\mu\nu}$, whose components are given by products of the matrix elements of the nuclear current J^μ between the initial and final nuclear states, i.e.,

$$W_{\mu\nu} = \sum_f \langle \Psi_f | J^\mu(\mathbf{q}) | \Psi_i \rangle \langle \Psi_i | J^{\nu\dagger}(\mathbf{q}) | \Psi_f \rangle \delta(E_i + \omega - E_f), \quad (2)$$

where ω and \mathbf{q} are the energy and momentum transfer, respectively. Similar models are used to calculate $W^{\mu\nu}$ in electron- and ν -nucleus scattering.

In a schematic representation of the nuclear response to the electroweak probe, different regions can be identified. At low energy transfer, below the threshold for the emission of a nucleon from the target, the response is dominated by discrete states, that can be treated in large model spaces. Above the continuum threshold there are giant resonance levels, collective excitations that can be described within the Random Phase Approximation (RPA). Then, a large broad peak occurs at about $\omega = q^2/2m_N$. Its position corresponds to the elastic peak in electron scattering by a free nucleon. In the region of the quasielastic (QE) peak the response is dominated by the single-particle (s.p.) dynamics and by one-nucleon knockout processes, where the interaction occurs on a quasifree nucleon which is emitted from the nucleus with a direct one-step mechanism. At higher energies mesons and nucleon resonances can be produced. For instance, at an excitation energy of ~ 300 MeV the Δ -peak corresponds to the first nucleon excitation.

Schematically, the response is the same for electron and neutrino scattering. However, the cross sections calculated for the (e, e') , (ν, ν') , (ν, e^-) , and $(\bar{\nu}, e^+)$ reactions on O^{16} in the same kinematic conditions within the continuum RPA have a quite different behavior [2, 4]. The difference is due to the different current in the electromagnetic and weak interactions: the neutrino cross sections are dominated by the axial vector term that does not contribute to electron scattering. As a consequence, it is necessary to be careful in relying on the fact that a model able to give a good description of electron scattering will give a good description of neutrino scattering. In spite of this warning, a model able to describe electron scattering data can be considered as a good basis to treat also ν -nucleus scattering.

A. Random Phase Approximation

Electron-nucleus and ν -nucleus cross sections calculated within the RPA are compared in Refs. [4, 5]. The RPA is an effective theory, aiming to describe the excitations of many-body

systems, that has been widely and successfully applied in nuclear physics over a wide range of excitation energies.

The RPA describes the nuclear excited states as a linear combination of particle-hole (ph) and hole-particle (hp) excitations. The combination coefficients for each state are obtained solving the secular RPA equations that contain s.p. energies and wave functions as input. They are generated by a Woods-Saxon potential whose parameters have been fixed to reproduce the energies of the levels close to the Fermi surface and the rms radii [4, 5]. The other input of the theory is the effective interaction, V^{eff} , that is an effective interaction in the medium. Calculations are compared in Ref. [4, 5] with various zero-range and finite-range interactions, in order to point out the sensitivity of the RPA results to the choice of V^{eff} .

RPA calculations are necessary to produce giant resonances and collective low-lying states. The results, however, strongly depend on the effective interaction used. Interactions equivalent from the spectroscopic point of view can produce different excited states. This indicates the limits of the RPA. In the evaluation of some observables, the use of effective interactions cannot substitute the explicit treatment of degrees of freedom beyond 1p-1h excitations. The use of quenching factors reduces the spreading of the results obtained with different interactions in the electron excitation and increases the spreading in the neutrino excitation. This is further evidence that electrons and neutrinos excite the same states in a different way. The uncertainty on the cross section is large for neutrinos of 20-40 MeV. These uncertainties have heavy consequences on the cross sections of low energy neutrinos. When the neutrino energy is above 50 MeV, the results are rather independent of the interaction and the inclusion of many-particle many-hole excitations reduces the RPA cross sections by a factor of $\simeq 10 - 15\%$.

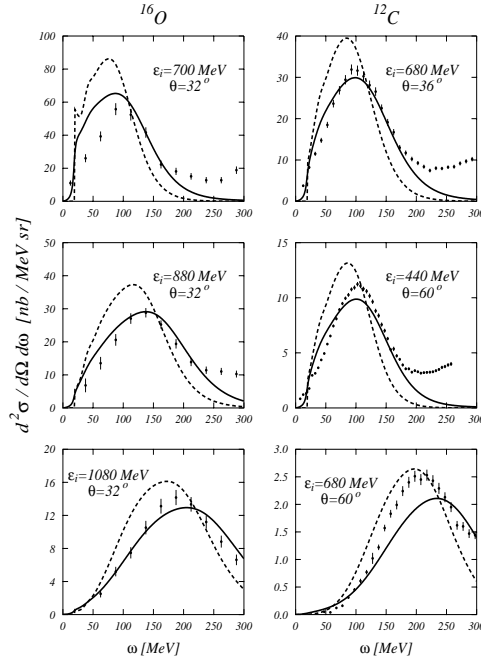


FIG. 1: $^{16}\text{O}(e,e')$ and $^{12}\text{C}(e,e')$ cross sections in the QE region. The MF results are shown by the dashed lines. The inclusion of FSI produces the full lines. Data from Ref. 7. (From Ref. 5).

In the QE region RPA effects are rather small when a finite-range V^{eff} is used [4, 5]. A zero-range interaction overestimates RPA effects. However, many-body effects beyond RPA are important,

as it is shown in Fig. 1, where QE $^{16}\text{O}(e,e')$ and $^{12}\text{C}(e,e')$ cross sections calculated within the mean-field (MF) model, i.e., setting $V^{\text{eff}} = 0$, are compared to data. In the QE region these many-body effects, which in the RPA language are described as many-particle many-hole excitations, are usually called Final-State Interactions (FSI). Different treatments of FSI are available in the literature. In Fig. 1 [4, 5] FSI are folded with a Lorentz function whose parameters are fixed by hadron scattering data [6] and give a redistribution of the strength that is essential to reproduce (e,e') data.

B. Nuclear Effects and FSI in the Quasielastic Region

In the QE region the nuclear response is dominated by one-nucleon knockout processes. A lot of theoretical and experimental work has been done to study the QE inclusive (e,e') and exclusive $(e,e'p)$ reactions [1, 8]. This work can be helpful to treat ν -nucleus scattering.

In the QE $\nu(\bar{\nu})$ -nucleus NC and CC scattering we assume that one nucleon is emitted

$$\nu(\bar{\nu}) + A \rightarrow \nu'(\bar{\nu}') + N + (A - 1) \quad \text{NC} \quad (3)$$

$$\nu(\bar{\nu}) + A \rightarrow l^-(l^+) + p(n) + (A - 1) \quad \text{CC} \quad (4)$$

In the NC scattering only the emitted nucleon can be detected. Thus, the cross section must be integrated over the energy and angle of the final lepton. Also the state of the residual $(A-1)$ -nucleus is not determined and the cross section is summed over all the available states of the residual nucleus. The same situation occurs for the CC reaction if only the outgoing nucleon is detected. The cross sections are therefore semi-inclusive in the hadronic sector and inclusive in the leptonic one and can be treated as an $(e,e'p)$ reaction where only the outgoing proton is detected. The exclusive CC process where, as in the case of $(e,e'p)$, the charged final lepton is detected in coincidence with the emitted nucleon can be considered as well. The inclusive CC scattering where only the charged lepton is detected can be treated with the same nuclear models used for the inclusive (e,e') scattering.

QE ν -nucleus scattering has been treated in Refs. [9, 10, 11] using the same relativistic models that were developed for the inclusive (e,e') and the exclusive $(e,e'p)$ reactions. These models include nuclear effects and FSI.

In the first order perturbation theory and in the Impulse Approximation (IA), the transition amplitude of the NC and CC processes where the outgoing nucleon is detected is described as the sum of terms similar to those appearing in the Relativistic Distorted Wave IA (RDWIA) for the $(e,e'p)$ knockout reaction. The amplitudes for the transition to a specific state n of the residual nucleus are obtained in a one-body representation

$$\langle n; \chi_{\mathbf{p}_N}^{(-)} | J^\mu(\mathbf{q}) | \Psi_i \rangle = \langle \chi_{\mathbf{p}_N}^{(-)} | j^\mu(\mathbf{q}) | \varphi_n \rangle \quad (5)$$

and contain three ingredients: the one-body nuclear weak current j^μ , the one-nucleon overlap $\varphi_n = \langle n | \Psi_i \rangle$, that is a s.p. bound state wave function whose normalization gives the spectroscopic factor, and the s.p. scattering wave function $\chi^{(-)}$ for the outgoing nucleon, that is eigenfunction of a complex optical potential describing the FSI between the outgoing nucleon and the residual nucleus.

Bound and scattering states are calculated with the same phenomenological ingredients used for the $(e,e'p)$ calculations. A pure SM description is assumed for the states n , i.e., n is a one-hole state in the SM and a sum over all the occupied SM states is carried out. In these calculations FSI are described by a complex optical potential whose imaginary part gives an absorption that reduces the cross sections by $\sim 50\%$. The imaginary part accounts for the flux lost in a particular

channel towards other channels. This approach is conceptually correct for an exclusive reaction, where only one channel contributes, but it would be conceptually wrong for an inclusive reaction, where all the channels contribute and the total flux must be conserved. For the semi-inclusive process where an emitted nucleon is detected, some of the reaction channels which are responsible for the imaginary part of the optical potential are not included in the experimental cross section and, from this point of view, it is correct to include the absorptive imaginary part of the potential.

In the inclusive scattering FSI can be treated in the Green's Function Approach (GFA), that was firstly applied to the QE (e,e') scattering in a nonrelativistic [14] and in a relativistic [13] framework, and then adapted to the CC scattering [15] and to the PVES [16] .

Recently, the GFA has been reformulated [17] , within a nonrelativistic framework, including antisymmetrization and nuclear correlations, that were neglected in previous applications. Correlations are included by means of realistic one-body density matrices. Their numerical effects on the (e,e') reaction are, however, small, within $\sim 5\%$ when only Short-Range Correlations (SRC) are included and within 10% when tensor correlations are added. These effects are in substantial agreement with those obtained in Ref. [18].

In the GFA the components of the nuclear response are written in terms of the s.p. optical model Green's function. This is the result of suitable approximations, such as the assumption of a one-body current and subtler approximations related to the IA. The explicit calculation of the Green's function can be avoided by its spectral representation, which is based on a biorthogonal expansion in terms of a non Hermitian optical potential \mathcal{H} and of its Hermitian conjugate \mathcal{H}^\dagger . In practice, the calculation requires matrix elements of the same type as the RDWIA ones in Eq. (5), but involves eigenfunctions of both \mathcal{H} and \mathcal{H}^\dagger , where the different sign of the imaginary part gives in one case an absorption and in the other case a gain of flux. Thus, the total flux is conserved and the imaginary part is responsible for the redistribution of the strength among different channels. This approach guarantees a consistent treatment of FSI in the exclusive and in the inclusive scattering.

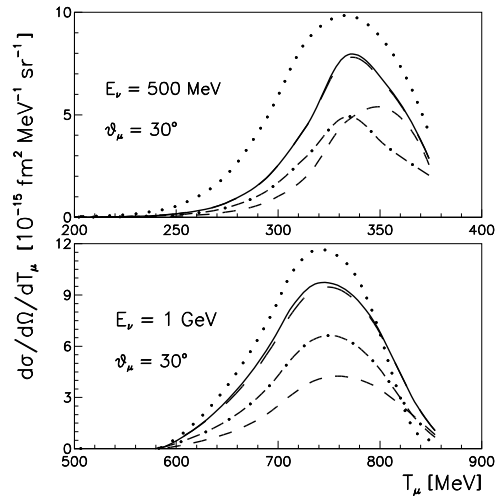


FIG. 2: The cross sections of the $^{16}\text{O}(\nu_\mu, \mu^-)$ reaction for $E_\nu = 500$ and 1000 MeV at $\theta_\mu = 30^\circ$ as a function of the muon kinetic energy T_μ . Results for GFA (solid) RPWIA (dotted), rROP (long-dashed) are compared. The dot-dashed lines give the contribution of the integrated exclusive reactions with one-nucleon emission. Short dashed lines give the cross sections of the $^{16}\text{O}(\bar{\nu}_\mu, \mu^+)$ reaction calculated within the GFA. (From Ref. 9).

An example of the role of FSI is displayed in Fig. 2, where the $^{16}\text{O}(\nu_\mu, \mu^-)$ cross sections calcu-

lated within the GFA are compared with the results of the Relativistic Plane Wave IA (RPWIA), where the plane wave approximation is assumed for the outgoing nucleon and FSI are neglected. The results obtained when only the real part of the Relativistic Optical Potential (rROP) is retained and the imaginary part is neglected are also shown in the figure. This approximation conserves the flux, but is inconsistent with the exclusive process. Although the use of a complex optical potential is conceptually important from a theoretical point of view, the very small differences given by the GFA and rROP results mean that the conservation of the flux is the most important condition in the present situation. The partial contribution given by the sum of all the integrated exclusive one-nucleon knockout reactions, also shown in the figure, is much smaller than the complete result. The difference is due to the spurious loss of flux produced by the absorptive imaginary part of the optical potential.

For the analysis of data a precise knowledge of ν -nucleus cross sections is needed, where theoretical uncertainties are reduced as much as possible. To this purpose, it is important to check the differences and the consistencies of the different models and the validity of the approximations used.

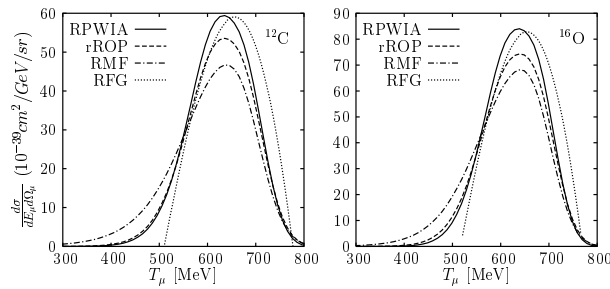


FIG. 3: The cross sections of the $^{12}\text{C}(\nu_\mu, \mu^-)$ and $^{16}\text{O}(\nu_\mu, \mu^-)$ reactions for $E_\nu = 1000$ MeV at $\theta_\mu = 45^\circ$ as a function of T_μ . The results of RPWIA (solid), rROP (dashed), RMF (dot-dashed), RFG (dotted) are compared. (From Ref. 19).

Different treatments of FSI are considered in Fig. 3 [19]. The RPWIA and rROP cross sections are compared with those of a Relativistic Mean Field (RMF) approach, where the distorted waves are calculated with the same potential used for the initial bound states. The results of the Relativistic Fermi Gas (RFG) are also displayed in the figure.

CC and NC cross sections calculated in the RPWIA and in the nonrelativistic PWIA are compared in Fig. 4. The differences are small at $E_\nu = 500$ MeV and somewhat larger at 1 GeV.

Relativistic and nonrelativistic models have been developed and applied in nuclear physics with electroweak probes. Relativistic effects have been widely investigated. They increase with the energy and for energies of about 1 GeV a fully relativistic model should be used. In order to account for these effects, relativistic corrections in the kinematics and in the current operators are often included in nonrelativistic models. Even with these corrections, however, a nonrelativistic approach cannot reproduce all the relativistic aspects in the dynamics of a relativistic one. Moreover, calculations are generally carried out in the two cases with different theoretical ingredients. Relativistic and nonrelativistic models have thus to be considered as different and alternative approaches. All the available models make use of approximations and have merits and shortcomings. Only a relativistic approach can fully account for relativistic effects. At present, however, nonrelativistic models may allow to include specific nuclear effects, e.g., due to correlations and two-body currents, in a more consistent and clear framework.

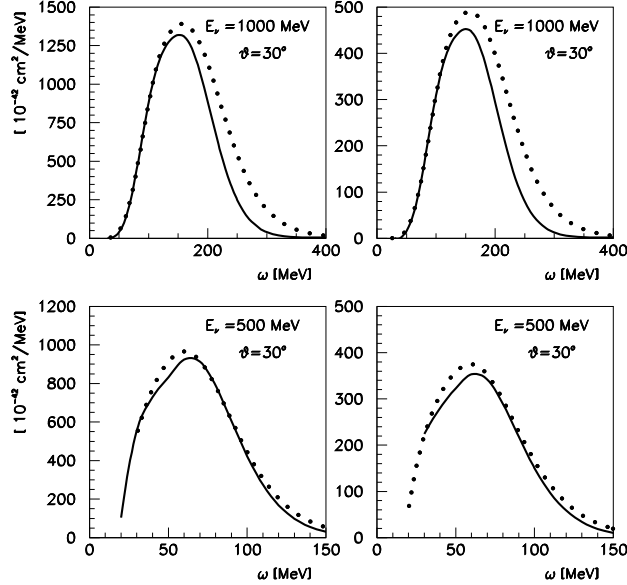


FIG. 4: The cross sections of the $^{16}\text{O}(\nu_e, e^-)$ (left panel) and $^{16}\text{O}(\nu, \nu')$ (right panel) reactions for $E_\nu = 500$ and 1000 MeV at $\theta = 30^\circ$. Solid lines: RWPIA (A. Meucci) dotted lines non relativistic PWIA (G. Co').

Nuclear correlations and FSI in electron and neutrino scattering off ^{16}O are considered in Refs. [20, 21, 22]. The approach is based on the nonrelativistic nuclear many-body theory and on the IA. In the IA the scattering process off a nuclear target reduces to the incoherent sum of elementary processes involving only one nucleon. For each term in the sum the cross section is factorized into the product of the elementary lepton-nucleon cross section and the nuclear spectral function, describing the momentum and energy distribution of nucleons in the target. The correlated spectral function of ^{16}O is obtained with a local density approximation in which nuclear matter results for a wide range of density values are combined with the experimental information from the $^{16}\text{O}(e, e'p)$ knockout reaction. FSI are treated within a Correlated Glauber Approximation (CGA), which rests on the premises that: i) the struck nucleon moves along a straight trajectory with constant velocity (eikonal approximation), ii) the spectator nucleons are seen by the struck particle as a collection of fixed scattering centers (frozen approximation). Under these assumptions, the propagator of the struck nucleon after the electroweak interaction is factorized in terms of the free space propagator and of a part that is related to the nuclear transparency measured in $(e, e'p)$. The cross section is written in the convolution form in terms of the IA cross section and of a folding function including FSI. A numerical example is presented in Fig. 5 for the $^{16}\text{O}(e, e')$ reaction. The model gives a good description of data in the region of the QE peak. FSI produce a shift and a redistribution of the strength leading to a quenching of the peak and to an enhancement of the tail. The FG model overestimates the data. The failure of the calculations to reproduce the data in the Δ -peak region is likely to be mostly due [23] to the poor knowledge of the neutron structure function at low Q^2 . The ability to yield quantitative predictions over a wide range of energies is critical to the analysis of neutrino experiments, in which the energy of the incident neutrino is not known, and must be reconstructed from the kinematics of the outgoing lepton.

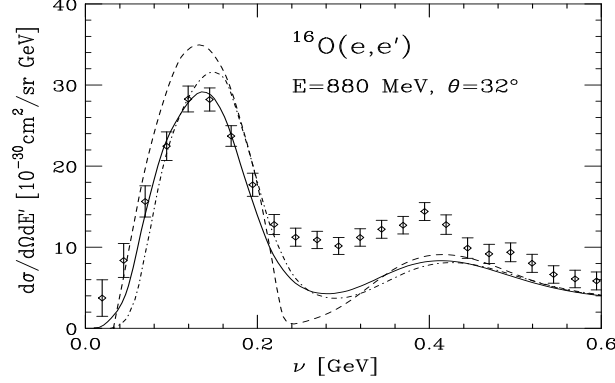


FIG. 5: Cross section of the $^{16}\text{O}(e,e')$ reaction at beam energy 880 MeV and electron scattering angle 32° . Dot-dashed line: IA, solid line: full calculation including FSI, dashed line: FG. Data from Ref. 7. (From Ref. 20).

III. TWO-BODY WEAK AXIAL CURRENT

Two-body Weak Axial Exchange Currents (WAECs) are considered in Refs. [24, 25]. The issue of the pion pair axial current is addressed in Ref. [24], showing how the interplay of the chiral invariance and the double-counting problem restricts uniquely its form. The complete treatment of the WAECs, including the heavy meson exchange contributions, that is, besides π -, ρ - ω - a_1 -exchange, is the main result of Ref. [25].

The Partial Conservation of the Axial Current (PCAC) reads

$$q_\mu \langle \Psi_f | j_{5\mu}^a(q) | \Psi_i \rangle = i f_\pi m_\pi^2 \Delta_F^\pi(q^2) \langle \Psi_f | m_\pi^a(q) | \Psi_i \rangle, \quad (6)$$

where the weak axial current $j_{5\mu}^a(q)$ is the sum of the one- and two-nucleon components

$$j_{5\mu}^a(q) = \sum_{i=1}^A j_{5\mu}^a(1, i, q_i) + \sum_{i < j}^A j_{5\mu}^a(2, i, j, q), \quad (7)$$

$m_\pi^a(q)$ is the pion source (the pion production/absorption amplitude). The wave functions $|\Psi_{i,f}\rangle$ describe the initial or final nuclear states, which are eigenfunctions of the Schrödinger equation with the nuclear Hamiltonian $H = T + V$, where V is the potential describing the interaction between nucleon pairs. From Eqs. (6) and (7), taking for simplicity $A = 2$, the following set of equations are obtained in the operator form for the one- and two-nucleon components of the axial current

$$\vec{q}_i \cdot \vec{j}_5^a(1, \vec{q}_i) = [T_i, \rho_5^a(1, \vec{q}_i)] + i f_\pi m_\pi^2 \Delta_F^\pi(q^2) m_\pi^a(1, \vec{q}_i), \quad i = 1, 2, \quad (8)$$

$$\begin{aligned} \vec{q} \cdot \vec{j}_5^a(2, \vec{q}) &= [T_1 + T_2, \rho_5^a(2, \vec{q})] + ([V, \rho_5^a(1, \vec{q})] + (1 \leftrightarrow 2)) \\ &\quad + i f_\pi m_\pi^2 \Delta_F^\pi(q^2) m_\pi^a(2, \vec{q}). \end{aligned} \quad (9)$$

If the WAECs are constructed in order to satisfy these conditions, the matrix element of the total current between the solutions of the nuclear equation of motion satisfies the PCAC.

The WAECs are constructed from an effective Lagrangian possessing the chiral symmetry and respecting the vector dominance model. The exchange amplitudes of range B ($B = \pi, \rho, \omega, a_1$) are derived as Feynman tree graphs and satisfy the PCAC. The currents are constructed from the

amplitudes, in analogy with the electromagnetic Meson Exchange Currents (MEC) [26], as the difference between the relativistic amplitudes and the first Born iteration of the weak axial one-nucleon current contribution to the two-nucleon scattering amplitude, satisfying the Lippmann-Schwinger equation.

For practical calculations a nonrelativistic reduction of the currents is performed. The nuclear wave functions are generated by the same One-Boson Exchange Potential (OBEP) of Eq. (9) and the same couplings and strong form factors as in the potential are applied in the WAECs. Consistent calculations are carried out employing the realistic OBE potentials OBEPQG [27], Nijmegen 93 and Nijmegen I [28].

The WAECs have been used to calculate ν - and $\bar{\nu}$ -deuteron disintegration cross sections at the typical solar neutrino energies. The results indicate that the main two-body effect comes from the Δ excitation and that the heavy-meson exchange contributions are of the same order of magnitude as the π -exchange one. The uncertainty of standard nuclear physics calculations has been reduced from 5-10% to about 3%.

IV. SCALING AND SUPERSCALING IN LEPTON-NUCLEUS SCATTERING

The analyses of ongoing and future neutrino experiments require reliable predictions of ν -nucleus cross sections. Any nuclear model should first be tested in comparison with electron scattering data. Sophisticated models have been developed to describe electron-nucleus scattering. In spite of all these efforts, however, the uncertainty due to the treatment of nuclear effects in different models is still high when compared with the required precision.

The analogies between ν -nucleus and electron-nucleus scattering suggest an alternative approach to extract model independent ν -nucleus cross sections from experimental electron-nucleus cross sections [29]. Instead of using a specific model, one can exploit the scaling properties of (e,e') data and i) extract a scaling function from (e,e') data, ii) invert the procedure to predict CC ν -nucleus cross sections.

This scaling approach [19, 29, 30, 31, 32] relies on the superscaling properties of the electron scattering data [33]. At sufficiently high momentum transfer a scaling function is derived dividing the experimental (e,e') cross sections by an appropriate single-nucleon cross section. This is basically the idea of the IA. If this scaling function depends only upon one kinematical variable, the scaling variable, one has scaling of first kind. If the scaling function is roughly the same for all nuclei, one has scaling of second kind. When both kinds of scaling are fulfilled, one says that superscaling occurs.

In the QE region the scaling variable is [29]

$$\psi_{\text{QE}} = \pm \sqrt{1/(2T_F) \left(q\sqrt{1+1/\tau} - \omega - 1 \right)}, \quad (10)$$

where T_F is the Fermi kinetic energy, $4m_N^2\tau = q^2 - \omega^2$ and the $- (+)$ sign corresponds to energy transfers lower (higher) than the QE-peak ($\psi = 0$).

An extensive analysis of electron scattering data [33] has shown that scaling of first kind is fulfilled at the left of the QEP and broken at its right, whereas scaling of second kind is well satisfied at the left of the peak and not so badly violated at its right. As a consequence, a scaling function f^{QE} can be extracted from the data.

The superscaling analysis has been extended to the first resonance peak [29]. The contribution of the Δ has been (approximately) isolated in the data by subtracting the QE scaling contribution from the total experimental cross sections. Then, the scaling function has been studied as a function

of a new scaling variable

$$\psi_{\Delta} = \pm \sqrt{1/(2T_F) \left(q\sqrt{\rho + 1/\tau} - \omega\rho - 1 \right)}, \quad (11)$$

where $\rho = 1 + (m_{\Delta}^2 - m_N^2)/(4\tau m_N^2)$. The results show that also in this region superscaling is satisfied and a second superscaling function, f^{Δ} , can be extracted from the data to account for the nuclear dynamics. Clearly this approach can work only at $\psi_{\Delta} < 0$, since at $\psi_{\Delta} > 0$ other resonances and the tail of the deep-inelastic scattering start contributing.

The two scaling functions can firstly be tested in comparison with (e,e') data and can then be used to predict ν -nucleus cross sections.

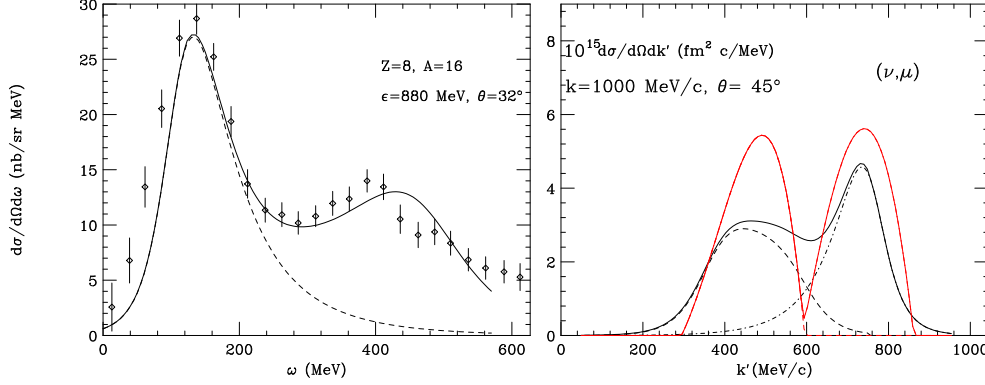


FIG. 6: Left panel: cross section of the $^{16}\text{O}(e,e')$ reaction. The solid line is obtained using f^{QE} and f^{Δ} , the dashed line using only f^{QE} . Data from Ref. 7. Right panel: cross section of the $^{12}\text{C}(\nu,\mu^-)$ reaction as a function of the muon momentum. Solid line: superscaling prediction; heavier line: RFG. The separate QE and Δ contribution are shown (dotted lines). (From Ref. 29).

In the left panel of Fig. 6 an example of the (e,e') cross section reconstructed by multiplying the empirical superscaling functions by the appropriate single-nucleon functions is shown in comparison with data. In this as well as in many other cases it turns out that typical deviations are 10% or less [29], thus confirming that the scaling approach offers a reliable description of the nuclear dynamics.

A numerical prediction for CC ν -scattering is displayed in the right panel of Fig. 6. The result obtained using the empirical scaling functions f^{QE} and f^{Δ} is compared with the result of the RFG model. The RFG cross section differs significantly from the scaling prediction, which lies somewhat lower and extends over a wider range in k' .

In the case of NC reactions, the kinematics are different from the ones of CC and (e,e') processes since the detected final state is the outgoing nucleon and the neutrino kinematic variables are integrated over. This implies an integration region in the residual nucleus variables which is different in the two cases and it is not obvious that the superscaling procedure, based on the analogy with inclusive electron scattering, is still valid. The scaling method is based on a factorization assumption which has to be tested numerically. The outcome is that the procedure can be applied also to NC reactions [31].

The properties of the empirical scaling functions should be accounted for by microscopic calculations. In particular, the asymmetric shape of f^{QE} should be explained. In Ref. [19] the scaling properties of different models (RPWIA, rROP, RMF) are verified. Superscaling is fulfilled to high accuracy in the QE region by the three descriptions of FSI considered. Then, the associated scaling functions are compared with the experimental scaling function. Only the RMF model is able

to reproduce the asymmetric shape of the experimental function. This result deserves further investigation.

More results on the scaling approach can be found in [34] .

V. ELECTROMAGNETIC REACTIONS ON FEW-NUCLEONS SYSTEMS

Electromagnetic reactions on few-body nuclei are investigated in Refs. [35, 36, 37]. The theoretical study of the electromagnetic structure of few-body nuclei requires the knowledge of the nuclear wave functions and the electromagnetic transition operators. For the low-energy observables considered in Ref. [35] and for processes involving two and three nucleons, accurate bound and scattering states are calculated using the pair-correlated Hyperspherical Harmonics (HH) method [38] from the Argonne v_{18} (AV18) two-nucleon [39] and Urbana IX (UIX) [40] or Tucson-Melbourne (TM) [41] three-nucleon interactions. For two- and three-nucleon interactions the nuclear electromagnetic current operator includes, in addition to the one-body terms, also two- and three-body terms. Different models for conserved two- and three-body currents are constructed using either meson exchange (ME) mechanisms or minimal substitution (MS) in the momentum dependence of the interactions. The connection between these two schemes is elucidated [35] .

The electromagnetic current operator must satisfy the Current Conservation Relation (CCR)

$$\mathbf{q} \cdot \mathbf{j}(\mathbf{q}) = [H, \rho(\mathbf{q})] , \quad (12)$$

where the Hamiltonian H contains two- and three-body interactions, v_{ij} and V_{ijk} , respectively. To lowest order in $1/m$, Eq. (12) separates into

$$\mathbf{q} \cdot \mathbf{j}_i(\mathbf{q}) = \left[\frac{\mathbf{p}_i^2}{2m}, \rho_i(\mathbf{q}) \right] , \quad \mathbf{q} \cdot \mathbf{j}_{ij}(\mathbf{q}) = [v_{ij}, \rho_i(\mathbf{q}) + \rho_j(\mathbf{q})] , \quad (13)$$

and similarly for the three-body current. The one-body current satisfies the CCR. It is rather difficult to construct conserved two- and three-body currents because H includes momentum and isospin dependent terms that do not commute with ρ .

The two-body current can be separated into model-independent (MI) and model-dependent (MD) parts. The MD current is purely transverse and is unconstrained by the CCR. The MI current has longitudinal and transverse components and is constrained by the CCR. The longitudinal part is constructed so as to satisfy the CCR. The MI currents from the momentum-independent terms of AV18 have been constructed following the ME scheme and satisfy the CCR. The currents from the momentum-dependent terms of the interaction obtained in the ME scheme do not strictly satisfy the CCR. If these currents are obtained in the MS scheme they satisfy the CCR. Both the ME and MS schemes can be generalized to calculate the three-body currents induced by a three-nucleon interaction.

Several electronuclear observables have been calculated [35] to test the model of the current operator. For the $A=3$ nuclear systems, cross sections and polarization observables in the energy range 0–20 MeV are compared with data and with earlier results [43] where the current operator retains only two-body terms, all of them obtained within the ME scheme, and the CCR is only approximately satisfied.

The differences with respect to the previous results are generally small, but for some of the polarization parameters measured in pd radiative capture, specifically the tensor polarizations T_{20} and T_{21} , where the exactly conserved currents resolve the discrepancies between theory and data obtained in Ref. [43]. An example is shown in Fig. 7.

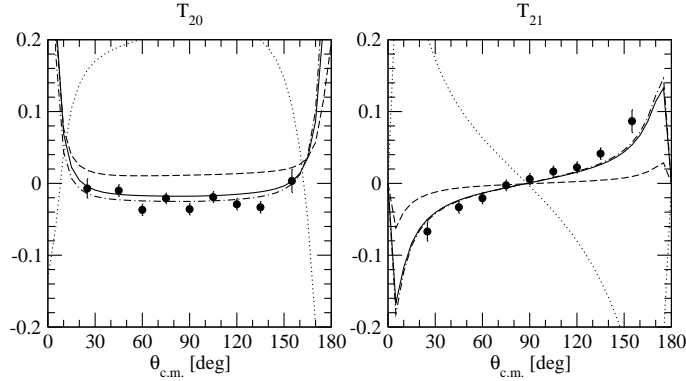


FIG. 7: Deuteron tensor polarization observables T_{20} and T_{21} for pd radiative capture at $E_{c.m.} = 2$ Me. The dotted curves include only the one-body current, the dashed curves are the results of Ref. 43, the dot-dashed curves are obtained in the long-wavelength-approximation (LWA), applying the Siegert theorem. The solid curves are the results of Ref. 35. Data from Ref. 42. (From Ref. 35).

An overall nice description has been reached for all the observables. Also, some small three-body currents effects are noticeable, which is an indication of the fact that if a Hamiltonian model with two- and three-nucleon interactions is used, then the model for the nuclear current operator should include the corresponding two- and three-body contributions [35].

A comparison with the $^3\text{He}(e,e'p)d$ [44] and $^4\text{He}(\vec{e},e'\vec{p})^3\text{H}$ [45] JLab data is presented in Refs. [36] and [37], respectively. Accurate bound state wave functions are still calculated within the HH method. The electromagnetic current operator includes one- and two-body terms. Since at the high energies of the JLab experiments a theory of the interaction and few-nucleon systems is not available, different treatments of FSI are used. In Ref. [36], a Glauber approximation is used, where the profile operator in the Glauber expansion is derived from a NN scattering amplitude, which retains its full spin and isospin dependence, and is consistent with phaseshift analyses of NN scattering data. In Ref. [37], a nonrelativistic optical potential is used including charge-exchange terms. In both cases a fair agreement with data is found. Of particular interest is the agreement obtained [37] for the ratio of transverse to longitudinal polarization transfers in the $^4\text{He}(\vec{e},e'\vec{p})^3\text{H}$ reaction. In the elastic process $\vec{e}p \rightarrow e\vec{p}$, the ratio is proportional to that of the electric to magnetic form factors of the proton, and a measurement in a nucleus by QE proton knockout can shed light, in principle, on the question of whether these form factors are modified in medium. Thus, the agreement found when free-nucleon electromagnetic form factors are used in the current operator [37] challenges the current interpretation of data in terms of medium-modified form factors.

VI. ELECTROMAGNETIC REACTIONS ON COMPLEX NUCLEI

Complementary polarization measurements suited to study nucleon properties in the nuclear medium are proposed in Ref. [46], where the general formalism of the $\vec{A}(\vec{e},e'\vec{p})B$ reaction is presented within the RPWIA. The simultaneous polarization of the target and the ejected proton provides information which is not contained in the $\vec{A}(\vec{e},e'p)B$ and $A(\vec{e},e'\vec{p})B$ reactions. The polarization transfer mechanism in which the electron interacts with the initial nucleon carrying the target polarization, making the proton exit with a fractional polarization in a different direction, is referred to as “skewed polarization”. Although difficult to measure, these new observables would provide information on nucleon properties complementing the results for the ratio of transverse to

longitudinal polarization transfers.

Proton emission induced by polarized photons of energies above the giant resonance region and below the pion production threshold is studied in Ref. [47]. With respect to $(e,e'p)$, a different kinematics is explored in the (γ,p) reaction. In fact, for a real photon the energy and momentum transfer are constrained by the condition $\omega = |\mathbf{q}|$, and only the high-momentum components of the nuclear wave function are probed. Moreover, the validity of the direct knockout mechanism, which is clearly stated for $(e,e'p)$, is questionable for (γ,p) , where important contributions are due to two-nucleon processes, such as those involving MEC [48, 49]. The sensitivity of various polarization observables in the $(\vec{\gamma},p)$ reaction to FSI, MEC, and SRC is investigated [47] using the same model [49] applied to calculate (γ,p) cross sections.

The sensitivity to FSI, MEC, and NN correlations, in particular SRC, are the same issues considered in the theoretical studies of electron- and photon-induced two-nucleon knockout [50, 51]. Since a long time these reactions have been devised as a preferential tool to investigate SRC [1]. In fact, direct insight into SRC can be obtained from the situation where the electromagnetic probe hits, through a one-body current, either nucleon of a correlated pair and both nucleons are then ejected from the nucleus. This process is entirely due to correlations. Additional complications have, however, to be taken into account, such as competing mechanisms, like contributions of two-body MEC and Δ isobar excitations, as well as the FSI between the two outgoing nucleons and the residual nucleus.

The calculated cross sections are sensitive to the different ingredients of the model and to their treatment. The role and relevance of competing reaction mechanisms and of different contributions is different in different reactions and kinematics. It is thus possible, in principle, with the help of theoretical predictions, to envisage appropriate situations where specific effects can be disentangled and separately investigated. Data from NIKHEF [52] and MAMI [53] for the exclusive $^{16}\text{O}(e,e'pp)^{14}\text{C}$ reaction confirmed the validity of the direct knockout mechanism and gave clear evidence of SRC for the transition to the ground state of ^{14}C . This important result, that was obtained from a close collaboration between experimentalists and theorists, means that further studies on these reactions would make it possible to disentangle SRC in experimental cross sections. From the experimental side, however, during the last few years only the results of a first measurement of the $^{16}\text{O}(e,e'pn)^{14}\text{N}$ reaction have been published [54]. From the theoretical side, the recent studies [50, 51] focussed on specific aspects of the theoretical models, such as a consistent treatment of different types of correlations in the two-nucleon wave function, the competing contribution of correlations and two-body currents, the uncertainties in the treatment of the Δ -current, the effects of FSI, whose consistent treatment requires in general a genuine three-body approach for the mutual interaction of the two nucleons and the residual nucleus.

The outcome of this work is that electromagnetic two-nucleon knockout contains a wealth of information on correlations and on the behavior of the Δ -current in a nucleus. The uncertainties in the treatment of the theoretical ingredients and the large number of parameters involved in the models make it difficult to extract clear and unambiguous information from one ideal kinematics. Data are therefore needed for electron- and photon-induced pp and pn emission and in various kinematics which mutually supplement each other. The choice of suitable conditions for the experiments and the interpretation of data require close collaboration between experimentalists and theorists.

I dedicate this report to the memory of Adelchi Fabrocini, who gave significant contributions to the study of correlations in electromagnetic reactions and with whom, during the years, I had

so many fruitful and pleasant conversations. I thank Franco Pacati for his valuable help and Giampaolo Co' for useful discussions.

-
- [1] S. Boffi, C. Giusti, F.D. Pacati, M. Radici, *Electromagnetic Response of Atomic Nuclei*, Oxford Studies in Nuclear Physics (Clarendon Press, Oxford, 1996); S. Boffi, C. Giusti, F.D. Pacati, *Phys. Rep.* **226**, 1 (1993).
 - [2] G. Co', in *Theoretical Nuclear Physics in Italy*, Proceedings of the 10th Conference on Problems in Theoretical Nuclear Physics, Cortona, 2004, edited by S. Boffi, A. Covello, M. Di Toro, A. Fabrocini, G. Pisent, S. Rosati (World Scientific, Singapore, 2005), p. 333.
 - [3] A. Meucci, C. Giusti, F.D. Pacati, these proceedings.
 - [4] A. Botrugno, G. Co', *Nucl. Phys.* **A761**, 200 (2005); *Eur. Phys. J.* **A24**, s1, 109 (2005).
 - [5] G. Co', *Nucl. Phys.* **B159** (Proc. Suppl.), 192 (2006); *Acta Phys. Polon.* **B37**, 2235 (2006).
 - [6] G. Co', K.F. Quader, R.D. Smith, J. Wambach, *Nucl. Phys.* **A485**, 61 (1988); C. Mahaux, N. Ngô, *Nucl. Phys.* **A378**, 205 (1982).
 - [7] M. Anghinolfi *et al.*, *Nucl. Phys.* **A602**, 405 (1996).
 - [8] O. Benhar, D. Day, I. Sick, nucl-ex/0603029.
 - [9] A. Meucci, C. Giusti, F.D. Pacati, nucl-th/0501047.
 - [10] A. Meucci, C. Giusti, F.D. Pacati, *Nucl. Phys.* **A773**, 250 (2006); *Acta Phys. Polon.* **B37**, 2279 (2006).
 - [11] C. Giusti, A. Meucci, F.D. Pacati, nucl-th/0607037.
 - [12] A. Meucci, C. Giusti, F.D. Pacati, *Phys. Rev.* **C64**, 014604 (2001).
 - [13] A. Meucci, F. Capuzzi, C. Giusti, F.D. Pacati, *Phys. Rev.* **C67**, 054601 (2003).
 - [14] F. Capuzzi, C. Giusti, F.D. Pacati, *Nucl. Phys.* **A524**, 681 (1991).
 - [15] A. Meucci, C. Giusti, F.D. Pacati, *Nucl. Phys.* **A739**, 277 (2004).
 - [16] A. Meucci, C. Giusti, F.D. Pacati, *Nucl. Phys.* **A756**, 359 (2005).
 - [17] F. Capuzzi, C. Giusti, F.D. Pacati, D.N. Kadrev, *Annals Phys.* **317**, 492 (2005).
 - [18] G. Co', A.M. Lallena, *Annals Phys.* **287**, 101 (2001).
 - [19] J.A. Caballero, J.E. Amaro, M.B. Barbaro, T.W. Donnelly, C. Maieron, J.M. Udías, *Phys. Rev. Lett.* **95**, 252502 (2005).
 - [20] O. Benhar, *Nucl. Phys.* **B139** (Proc. Suppl.), 15 (2005).
 - [21] O. Benhar, N. Farina, *Nucl. Phys.* **B139** (Proc. Suppl.), 230 (2005); O. Benhar, N. Farina, H. Nakamura, M. Sakuda, R. Seki, *Phys. Rev.* **D72**, 053005 (2005); *Nucl. Phys.* **B155** (Proc. Suppl.), 155 (2006).
 - [22] O. Benhar, *Nucl. Phys.* **B159** (Proc. Suppl.), 168 (2006); *Acta Phys. Polon.* **B37**, 2243 (2006).
 - [23] O. Benhar, D. Meloni, hep-ph/0604071; hep-ph/0610403.
 - [24] B. Mosconi, P. Ricci, E. Truhlík, *Eur. Phys. J.* **A25**, 283 (2005).
 - [25] B. Mosconi, P. Ricci, E. Truhlík, *Eur. Phys. J.* **A27**, s1, 67 (2006); *Nucl. Phys.* **A772**, 81 (2006).
 - [26] J. Adam, Jr., E. Truhlík, D. Adamová, *Nucl. Phys.* **A494**, 556 (1989).
 - [27] R. Machleidt, *Advances in Nuclear Physics*, **19**, 189 (1989); P. Obersteiner, W. Plessas, E. Truhlík, in *Proceedings of the XIII International Conference on Particles and Nuclei, Perugia 1993* edited by A. Pascolini, (World Scientific, Singapore, 1994), p. 430.
 - [28] V.G.J. Stoks, R.A.M. Klomp, C.P.F. Terheggen, J.J. de Swart, *Phys. Rev.* **C49**, 2950 (1994).
 - [29] J.E. Amaro, M.B. Barbaro, J.A. Caballero, A. Molinari, I. Sick, *Phys. Rev.* **C71**, 015501 (2005).
 - [30] J.E. Amaro, M.B. Barbaro, J.A. Caballero, T.W. Donnelly, C. Maieron, *Phys. Rev.* **C71**, 065501 (2005).
 - [31] J. E. Amaro, M. B. Barbaro, J.A. Caballero, T. W. Donnelly, *Phys. Rev.* **C73**, 035503 (2006).
 - [32] M. B. Barbaro, J. E. Amaro, J.A. Caballero, T. W. Donnelly, A. Molinari, I Sick, *Nucl. Phys.* **B155** (Proc. Suppl.), 257 (2006); M.B. Barbaro, nucl-th/0602011; M. B. Barbaro, J. E. Amaro, J.A. Caballero, T.W. Donnelly, nucl-th/0609057; A.N. Antonov *et al.* *Phys. Rev.* **C74**, 054603 (2006).
 - [33] W.M. Alberico, A. Molinari, T.W. Donnelly, E.L. Kronenberg, J.W. Van Orden, *Phys. Rev.* **C38**, 1801 (1988); D.B. Day, J.S. MacCarthy, T.W. Donnelly, I. Sick, *Ann. Rev. Nucl. Part. Sci.* **40**, 357 (1990); T.W. Donnelly, I. Sick, *Phys. Rev.* **C60**, 065502 (1999); *Phys. Rev. Lett.* **82**, 3212 (1999); C. Maieron, T. W. Donnelly, I. Sick, *Phys. Rev.* **C65**, 025502 (2002).
 - [34] M. Martini, these proceedings.
 - [35] L.E. Marcucci, M. Viviani, R. Schiavilla, A. Kievsky, S. Rosati, *Eur. Phys. J.* **A24**, s1, 95 (2005); *Phys.*

- Rev.* **C72**, 014001 (2005).
- [36] R. Schiavilla, O. Benhar, A. Kievsky, L.E. Marcucci, M. Viviani, *Phys. Rev.* **C72**, 064003 (2005).
 - [37] R. Schiavilla, O. Benhar, A. Kievsky, L.E. Marcucci, M. Viviani, *Phys. Rev. Lett.* **94**, 072303 (2005).
 - [38] A. Kievsky, M. Viviani, S. Rosati, *Nucl. Phys.* **A551**, 241 (1993); *Nucl. Phys.* **A577**, 511 (1994); A. Kievsky, S. Rosati, M. Viviani, *Phys. Rev.* **C64**, 024002 (2001).
 - [39] R.B. Wiringa, V.G.J. Stoks, R. Schiavilla, *Phys. Rev.* **C51**, 38 (1995).
 - [40] B.S. Pudliner, V.R. Pandharipande, J. Carlson, R.B. Wiringa, *Phys. Rev. Lett.* **74**, 4396 (1995).
 - [41] S.A. Coon, *et al.* *Nucl. Phys.* **A317**, 242 (1979).
 - [42] M.K. Smith, L.D. Knutson, *Phys. Rev. Lett.* **82**, 4591 (1999).
 - [43] M. Viviani, A. Kievsky, L.E. Marcucci, S. Rosati, R. Schiavilla, *Phys. Rev.* **C61**, 064001 (2000).
 - [44] M.M. Rvachev *et al.*, *Phys. Rev. Lett.* **94**, 192302 (2005).
 - [45] S. Strauch *et al.*, *Phys. Rev. Lett.* **91**, 052301 (2003).
 - [46] J.E. Amaro, M.B. Barbaro, J.A. Caballero, *Annals Phys.* **319**, 123 (2005).
 - [47] M. Anguiano, G. Co', A.M. Lallena, *Phys. Rev.* **C74**, 044603 (2006).
 - [48] C. Giusti, F.D. Pacati, *Phys. Rev.* **C66**, 034610 (2002).
 - [49] M. Anguiano, G. Co', A.M. Lallena, S.R. Mokhtar *Annals Phys* **296**, 235 (2002).
 - [50] M. Anguiano, G. Co', A.M. Lallena, *J. Phys* **G29**, 1119 (2003); *Nucl. Phys* **A744**, 168 (2004).
 - [51] C. Barbieri, C. Giusti, F.D. Pacati, W.H. Dickhoff, *Phys. Rev.* **C70**, 014606 (2004); M. Schwamb, S. Boffi, C. Giusti, F.D. Pacati, *Eur. Phys. J.* **A20**, 233 (2004); M. Schwamb, C. Giusti, F.D. Pacati, S. Boffi, *Eur. Phys. J.* **A26**, 209 (2005); C. Giusti, *BGNS Transactions* **10** n.2 136, (2005).
 - [52] C.J.G. Onderwater *et al.*, *Phys. Rev. Lett.* **78** 4893 (1997); **81**, 2213 (1998); R. Starink *et al.*, *Phys. Lett.* **B474**, 33 (2000).
 - [53] G. Rosner, *Prog. Part. Nucl. Phys.* **44**, 99 (2000).
 - [54] D.G. Middleton *et al.*, *Eur. Phys. J.* **A29**, 261 (2006).